Biosensors and Bioelectronics 138 (2019) 111322

Contents lists available at ScienceDirect

Biosensors and Bioelectronics

journal homepage: www.elsevier.com/locate/bios

The construction of *Mycobacterium tuberculosis* 16S rDNA MSPQC sensor based on Exonuclease III-assisted cyclic signal amplification

Jialin Zhang, Ji Huang, Fengjiao He*

State Key Laboratory of Chemo/Biosensing and Chemometrics, College of Chemistry and Chemical Engineering, Hunan University, Changsha, 410082, PR China

ARTICLE INFO

Keywords:
MSPQC
Exo III
16S rDNA
Mycobacterium tuberculosis

ABSTRACT

Tuberculosis caused by *Mycobacterium tuberculosis* (*M. tuberculosis*) remains one of the most serious infectious diseases all over the world. The key to reduce the spread and mortality rate of tuberculosis is to develop faster and more sensitive approaches for detection of *M. tuberculosis*. However, current detection methods can not meet the requirements of rapid clinical *M. tuberculosis* detection in terms of detection time. Herein, a new 16S rDNA multichannel series piezoelectric quartz crystal (MSPQC) sensor based on Exonuclease III (Exo III)-aided target recycling has been developed for rapid detection of *M. tuberculosis*. The specific 16S rDNA fragment of *M. tuberculosis* was used as biomarker, DNA capture probes complementary to the biomarker were designed and modified on the surface of AuNPs. The Exo III which could recognise hybrid duplexes and selectively digest DNA capture probe was used to assist digestion cycle by digesting DNA capture probe and releasing the intact target fragment. After all DNA probes loading on the surface of AuNPs were removed, the surface of AuNPs was exposed and conductive connection was formed between the nanogap network electrode by self-catalytic growth of exposed AuNPs in the glucose and $HAuCl_4$ solution. This resulted in sensitive response of *M. tuberculosis* sensor and *M. tuberculosis* was detected by recording this response. The limit of detection (LOD) of the method was 20 CFU/mL and the detection time was less than 3 h. It was expected to be widely used in detection methods of *M. tuberculosis*.

1. Introduction

Tuberculosis, caused by the widely spread pathogen *M. tuberculosis*, is one of the major public health problems in the world, which causing about 1.8 million deaths in 2015 (World Health Organization, 2016). At present, the traditional approaches for tuberculosis diagnosis mainly include sputum smear microscopy (N'guessan et al., 2016), chest X-ray (Chu et al., 2019) and bacterium culture examination (Chen et al., 2018a). However, sputum smear microscopy has poor sensitivity and low positive rate of 50%–60% (Li et al., 2014). Clinical chest X-ray has poor specificity for tuberculosis diagnosis and fails in early detection (Yan et al., 2017). For bacterium culture examination, it takes about 4–6 weeks to yield satisfied results (Sypabekova et al., 2019). The BACTEC system has shortened the detection time to 10 days, but it still can not meet the needs of early clinical diagnosis (Mi et al., 2012). Therefore, the topic for rapid detection of *M. tuberculosis* is still concerned by the researchers. Recently several new alternative methods have been reported for detection of *M. tuberculosis* (Gupta and Kakkar, 2018). Though with rapid and sensitivity advantages, the methods such as real-time polymerase chain reaction (PCR), surface plasmon resonance (SPR) and fluorescence are relatively expensive. The immunological detection technology based on monoclonal antibody has high selectivity and specificity, but it is limited because the monoclonal antibodies are often difficult to obtain and expensive. The colorimetric method is simple and low-cost, but it has poor sensitivity in the detection of complex samples. Therefore, there is a need to develop a simple, low-cost, rapid and sensitive method for early detection of *M. tuberculosis*.

The 16S rDNA sequence structure consists of the constant region and variable region (Chung et al., 2013). The constant region is highly conserved and suitable for universal detection of bacteria. The variable region sequences vary with different bacterium, which are suitable for species typing, especially have advantages in isolation and identification of caustic and slow-growing bacteria. The methods such as quantitative real-time PCR (qPCR) (Hünniger et al., 2015), fluorescence (Shi et al., 2017) and sequencing (Wang et al., 2014) based on 16S rDNA sequence detection have been used for rapid and sensitive detection of bacteria. However, these methods are expensive, which restricted their applications in developing countries (Das et al., 2018).

Recently, MSPQC sensors have received extensive attention in the

* Corresponding author.
E-mail address: fengjiao87799232@hotmail.com (F. He).

https://doi.org/10.1016/j.bios.2019.111322
Received 28 March 2019; Received in revised form 5 May 2019; Accepted 12 May 2019
Available online 14 May 2019
0956-5663/

field of pathogen diagnosis due to the promising advantages of high sensitivity, low cost and easy operation (Lakshmanan et al., 2014; Zhang et al., 2017; Shi et al., 2019). A series of *M. tuberculosis* sensors based on MSPQC system were constructed for sensitive detection of *M. tuberculosis* (Ren et al., 2008; He et al., 2016). However, the target of these methods is culture-based metabolite or antigen CFP10-ESAT6, it still can not overcome the drawbacks of culture and immunoassay.

In this study, a new 16S rDNA MSPQC sensor based on Exo III-assisted target cycle was developed for rapid detection of *M. tuberculosis* stable attenuated strain H37Ra. The sensor has the advantages of low cost, high sensitivity and specificity. The LOD of the sensor was 20 CFU/mL and the detection time was less than 3 h. The proposed method was applied to the detection of *M. tuberculosis* in simulated sputum samples with satisfactory results.

2. Material and methods

2.1. Reagents and materials

2.1.1. Bacteria and medium

Escherichia coli (*E. coli*), *Staphylococcus aureus* (*S. aureus*), *Pseudomonas aeruginosa* (*P. aeruginosa*) and *M. tuberculosis* (H37Ra) were obtained from the National Institute for the Control of Pharmaceutical and Biological Products. *Mycobacterium smegmatis* (*M. smegmatis*) and BCG vaccine were purchased from Institute of Microbiology Chinese Academy of Sciences. The concentrations of these strains were detected by McFarland's turbidimetric assay. The culture medium was prepared by mixing 95 mL nutrimental medium, 5 mL bovine serum albumin-glucose solution and 0.3 mL catalase solution.

Nutrimental medium was prepared by adding ammonium sulfate (0.5 g), sodium hydrogen phosphate (2.5 g), potassium dihydrogen phosphate (1 g), magnesium sulfate (0.05 g), zinc sulfate (0.001 g), calcium chloride(0.0005 g), copper sulfate (0.001 g), sodium glutamate (0.5 g), sodium citrate (0.1 g), pyridoxine hydrochloride (0.001 g), biotin (0.0005 g), ferric ammonium citrate (0.04 g) and Tween-80 (0.5 g) to 1 L of distilled water. Medium was separated into 95 mL and autoclaved at 120 °C for 15 min.

Bovine serum albumin-glucose solution was prepared by adding bovine serum albumin (50 g) and glucose (20 g) to 1 L of distilled water. Catalase solution was prepared by adding catalase (10 mg) to 10 mL of deionized water. The two mediums were respectively sterilized by passing through a 0.22 mm sterilized Millipore membrane filters.

The sterile sputum samples were spiked with 10^3 CFU/mL of *M. tuberculosis* to obtain simulated positive sputum samples, and sterile sputum samples were regarded as the negative samples.

2.1.2. Reagents

AvaII restriction endonuclease, MslI restriction endonuclease enzyme and Exonuclease III were purchased from New England Biolabs (NEB). The Au interdigital electrode (Au-IDE) was purchased from Dalian Institute of Chemical Physics. 5% Chelex-100 solution (5 g Chelex-100 in 100 mL 0.5% SDS, 1% Tween 20 and 1% NP40 buffer). Hybridization and washing buffered solution (pH 8.5, 10 mM Tris-HCl, 1.0 mM EDTA and 0.10 M NaCl solution).

2.1.3. Sequence

The following oligonucleotides were prepared by Sangon Biotech. Co., Ltd. (Shang hai, China), and the detailed sequences were shown in Table 1.

2.1.4. Apparatus

The equipments included high-resolution transmission electron microscope JEM-3010 (Japan Electronics Corporation, Japan), a Fluorolog3 fluorimeter (Horiba, Kyoto, Japan), and HP4192A impedance analyzer (Hewlett Packard, USA). MSPQC was made in our laboratory. Its schematic diagram was showed in Fig. S1.

Table 1
The detailed oligonucleotide sequences used in this work.

Oligonucleotide Type	Sequences
DNA capture probe	5′–S- TGCTACCCACAGCCGGTTAGG-S–3′
16S rDNA fragment	5′–CCTAACCGGCTGTGGGTAGCAGACCTCACCT–3′
Single-base mismatch	5′–CCTATCCGGCTGTGGGTAGCAGACCTCACCT–3′
Three-bases mismatch	5′–CCTATCCAGCTGCGGGTAGCAGACCTCACCT–3′
Five-bases mismatch	5′–CCTATCCAGCTGCGGCTATCAGACCTCACCT–3′
Non-match	5′–ATCTTTGACAGACCACGCTATGACCTCACCT–3′

2.2. Detection of M. tuberculosis

2.2.1. Extraction of specific 16S rDNA fragments

1 mL of *M. tuberculosis* H37Ra solution (10^6 CFU/mL) was added to centrifuge tube and centrifuged for 5 min at 8 K rpm at 4 °C. The supernatant was discarded, followed by adding 20 μL of 5% Chelex-100 solution to the centrifuge tube. After mixed thoroughly, the solution was treated for 10 min under 100 °C water bath and then for 1 min under ice bath. The centrifugation was carried out at 12 K rpm for 10 min at room temperature and the supernatant solution was transferred to Cutsmart Buffer. 1 μL of AvaII restriction enzyme and 1 μL of MslI restriction enzyme were added, and the fragments solution was obtained after incubating at 37 °C for 10 min.

2.2.2. Extraction of M. tuberculosis 16S rDNA fragments in simulated sputum samples

6 mL of 4% sodium hydroxide solution was added to the centrifuge tube containing 3 mL of simulated sputum sample solution. After sealed with a screw cap, the tube was oscillated on the scroll oscillator for 1 min, followed by staying for 15 min at room temperature to ensure the sputum fully homogenized. 9 mL of 67 mM sterile phosphate buffer (pH 6.8) was added into the tube and mixed thoroughly. The centrifugation was carried out at 4 K rpm for 15 min and the supernatant was abandoned. The sediment was then washed with 15 mL of sterile PBS buffer and M7H9 medium, thus the detection sample solution was prepared for use. The 16S rDNA fragments were extracted using the method described in Section 2.2.1.

2.2.3. Detection of 16S rDNA fragments

The 16S rDNA fragments solution was added to the detecting cell containing AuNPs-DNA network electrode (See Section S1 in the Supporting information), followed by adding 10 μL of Exo III (2.5 U/μL) into the electrode and incubating at 25 °C for 1 h. The electrode was thoroughly cleaned using the washing buffer (pH 9.5) and dried under nitrogen flow. The medium solution containing 150 mM glucose and 1 mM $HAuCl_4$ (pH 7.2) was added to the electrode and maintained for 40 min at 38 °C. The frequency shift response in this period was recorded under mild environment with the MSPQC system. Datas were from the average of three measurements.

3. Results and discussion

3.1. The constructed strategy of MSPQC sensor

The constructed strategy of the MSPQC sensor was shown in Fig. 1A. The AuNPs-DNA nanogap network electrode modified with DNA capture probes could specifically capture the 16S rDNA fragment of *M. tuberculosis* to form a DNA duplex. The Exo III recognized the duplex region and selectively cleaved the DNA capture probe on the surface of AuNPs, releasing the intact target fragment (Gao and Li, 2013; Xiong et al., 2015; Qu et al., 2017). The target hybridized with the next DNA capture probe on the surface of AuNPs and further round of cleavage was initiated. The cycle continued until all DNA probes loading on the surface were removed, thus the surface of AuNPs was exposed. When glucose and $HAuCl_4$ solution were added to the detecting cell, self-

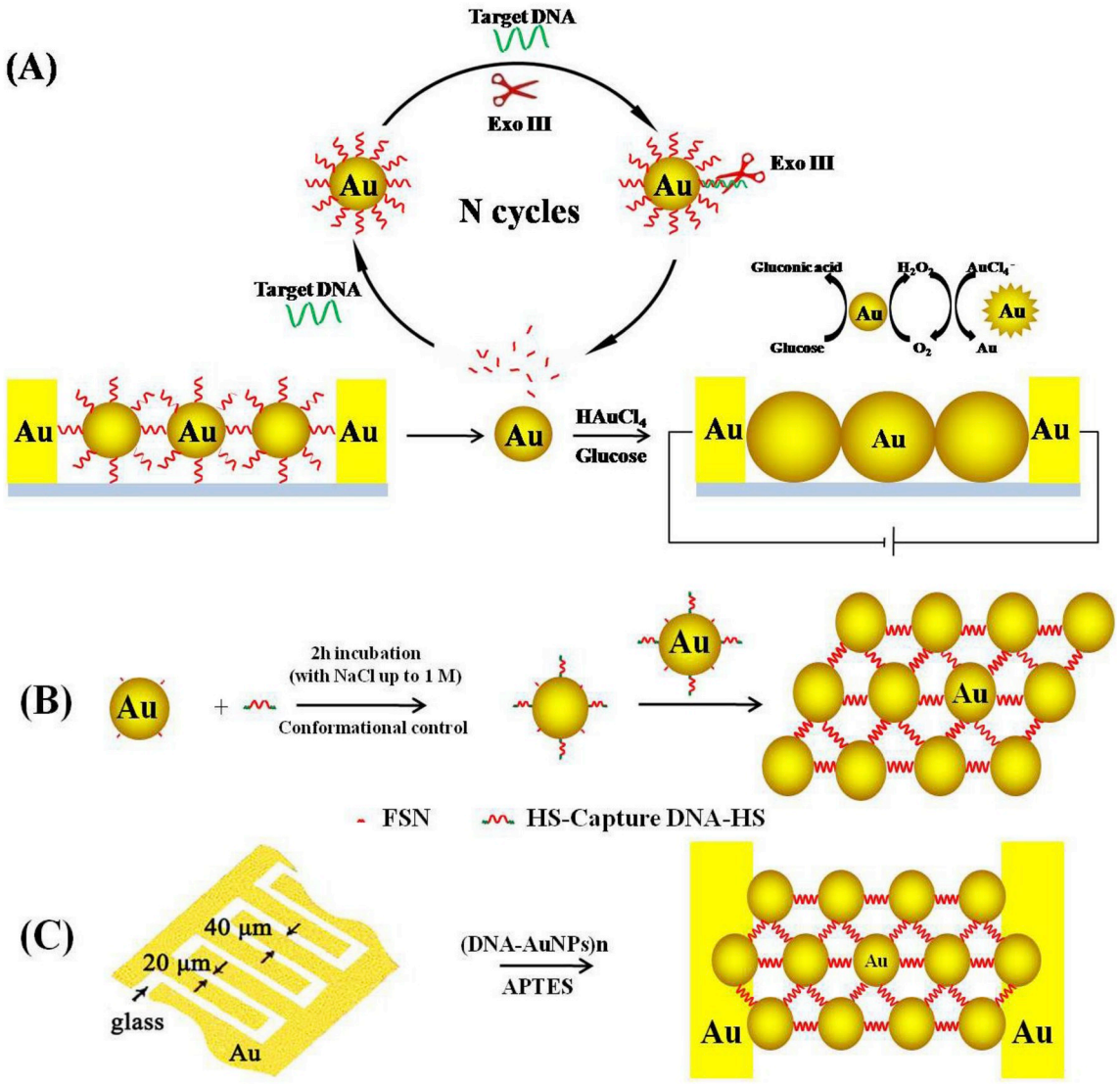

Fig. 1. The constructed strategy of 16S rDNA MSPQC sensor. (A) Sensing scheme of the sensor. (B) Preparation method of AuNPs-DNA conjugates. (C) The preparation of AuNPs-DNA network electrode.

catalytic growth of the exposed AuNPs which assembled on the substrate of electrode could induce the enlargement of AuNPs diameters (Zheng et al., 2011; Comotti et al., 2004). Conductive connection was formed between the electrodes and caused a sensitive frequency shift response of MSPQC sensor (see Section S2 in the Supporting information). Thus the presence of *M. tuberculosis* was detected.

The preparation of nanogap network electrode was shown in Fig. 1B–C, DNA probe with thiol groups at both terminals was connected the adjacent AuNPs to form AuNPs-DNA conjugates (Fig. 1B). After dropped on the substrate of 20 μm interdigitated gap of Au-IDE and dried with nitrogen, DNA capture probe-linked AuNPs-DNA nanogap network electrode was formed (Fig. 1C). In a sense, gold nanoparticles were equal to the nano-electrodes. The preparation process was easy and cheap. The nanogap network electrodes showed higher surface areas and better ability for target acquisition. The label-free method using Exo III-assisted target recycling could recycle the low concentration 16S rDNA target fragments of *M. tuberculosis*, which amplified the detectable signal limit and detected *M. tuberculosis* in a large analytical range, thus dramatically enhanced the sensitivity of detection of *M. tuberculosis*.

3.2. Selection of the 16S rDNA target sequences and design of capture probe

The species-specific region of 16S rDNA sequences of *M. tuberculosis* was verified based on alignments of the 16S region using Vector NTI 9.0 software package. Primer Premier 5.0 software was used to optimize the length by considering the suitable restriction endonuclease sites and the thermodynamic properties like the melting temperature and stable secondary structures against the species-specific variable region of the sequence. The screening target was blasted in the NCBI Web site and the result showed the highest similarity to 16S rDNA sequences of *M. tuberculosis* culture collection reference strains. Therefore, the suitable target fragment was selected for *M. tuberculosis* detection (see Table 1).

The DNA capture probe was designed 10 bases shorter than the complementary 16S rDNA fragment at its 3′-termini, thus the sequence of DNA capture probe was obtained (see Table 1). As the sequence of target fragment was 10 bp more than the capture probe, only capture probe was being digested by Exo III in the next digestion cycle steps (Chen et al., 2018b; Zhou and Li, 2015; Lu et al., 2017).

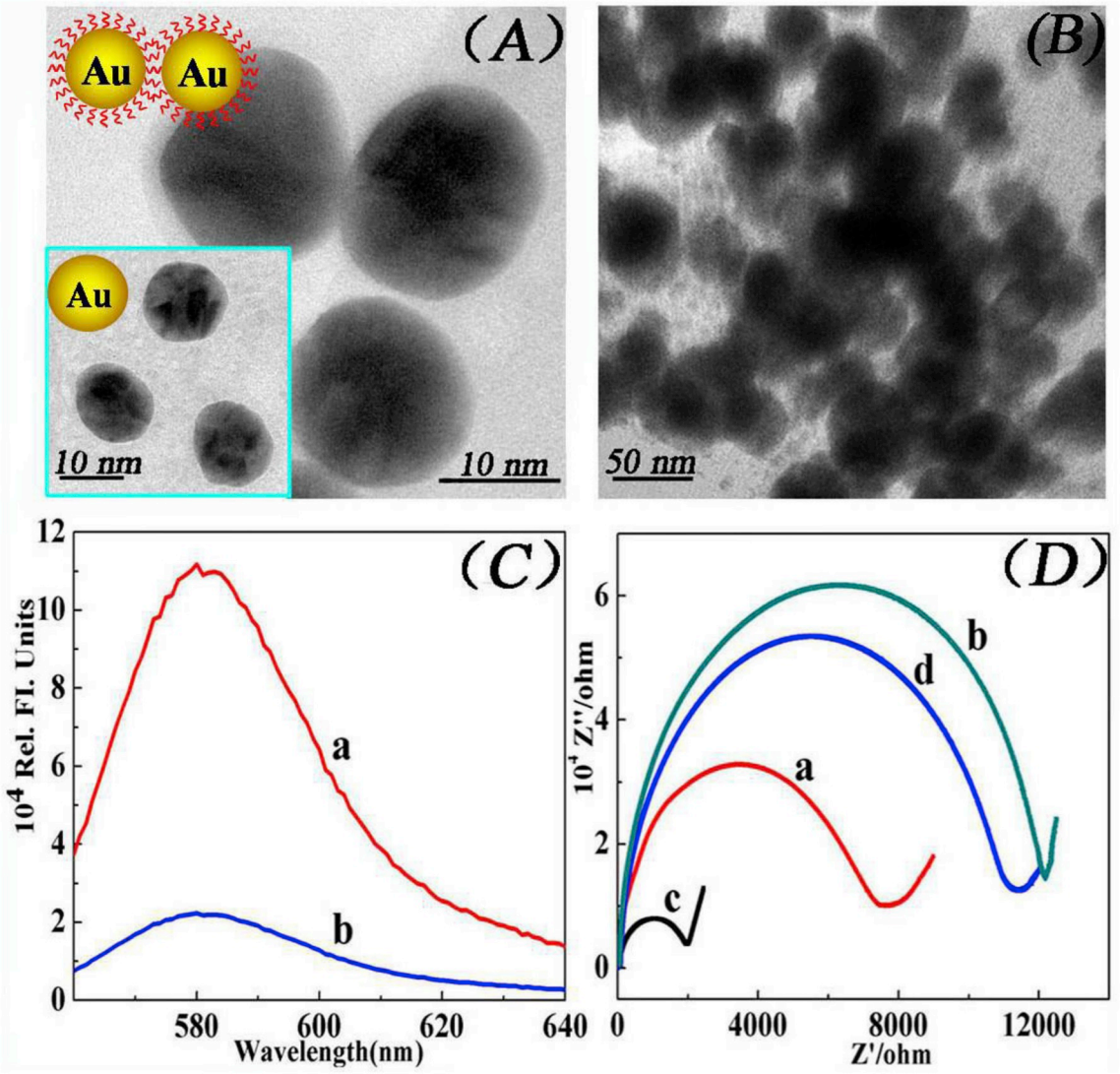

Fig. 2. (A) TEM images of AuNPs-DNA conjugates and bare AuNPs (inset). (B) TEM image of self-catalytic growth of exposed AuNPs in the glucose and $HAuCl_4$ solution. (C) Fluorescence emission recorded at 579 nm for AuNP@ssDNA:16S rDNA before (b) and after (a) incubation with Exo III (D) Electrochemical impedance spectroscopy: (a) bare Au-IDE, (b) AuNPs-DNA network electrode, (c) self-catalytic growth of exposed AuNPs, 10 pM target DNA, 2.5 U/μL Exo III, the glucose and $HAuCl_4$ solution, (d) no target DNA, 2.5 U/μL Exo III, the glucose and $HAuCl_4$ solution.

3.3. Verification of key steps in sensing process of MSPQC sensor

3.3.1. TEM characterization of AuNPs self-catalytic growth

Transmission electron microscopy (TEM) of AuNPs-DNA conjugates and self-catalytic growth of exposed AuNPs was shown in Fig. 2A and Fig. 2B, respectively. As shown in Fig. 2A, compared with bare gold nanoparticles (illustrations), the distance between adjacent AuNPs was closer due to the DNA connection. As shown in Fig. 2B, due to the self-catalytic growth of exposed AuNPs in glucose and $HAuCl_4$ solution, conductive connection was formed between the interrupted AuNPs.

3.3.2. Fluorescence experiment to verify Exo III-aided target recycling

The Exo III-assisted target recycling was verified by fluorescence experiment of TAMRA-labeled AuNP@ssDNA. Specifically, TAMRA was modified at the 5′ end of DNA capture probes loading on AuNPs, after the hybridization between DNA probes and the target, Exo III was added and selectively cleaved the DNA probe. The released intact target fragment hybridized with the next DNA probe and thus initiating the next round of probe digestion until all DNA probes have been digested. Before enzyme digestion cycle, TAMRA was closed to AuNPs through DNA probes, the effect of AuNPs on the quenching of fluorescent groups made the fluorescence signal weak in the suspension. After the enzyme digestion cycle, TAMRA was far away from the AuNPs, which enhanced the fluorescence signal. As shown in Fig. 2C, it can be clearly seen that the fluorescence at 579 nm increased by 81.8% after the enzyme digestion cycle. The result indicated that Exo III-assisted target recycling has been carried out.

3.3.3. Electrochemical impedance characterization of the electrode surface

The impedance characteristics of electrode surface changes were studied by using an HP-4192A LF impedance analyzer. As shown in Fig. 2D, the diameter of the semicircle of AuNPs-DNA network electrode (curve b) was larger than that of the Au-IDE (curve a), which indicated that the AuNPs-DNA network was formed on the surface of Au-IDE. The diameter of the semicircle of the electrode after self-catalytic growth of exposed AuNPs (curve c) was markedly smaller than that of the AuNPs-DNA network electrode (curve b) and the blank (no target, curve d), indicating that conductive connection was formed between the nanogap network electrode after self-catalytic growth of the exposed gold NPs. This impedance difference indicated that the constructed MSPQC sensor could improve the sensitivity of *M. tuberculosis* detection.

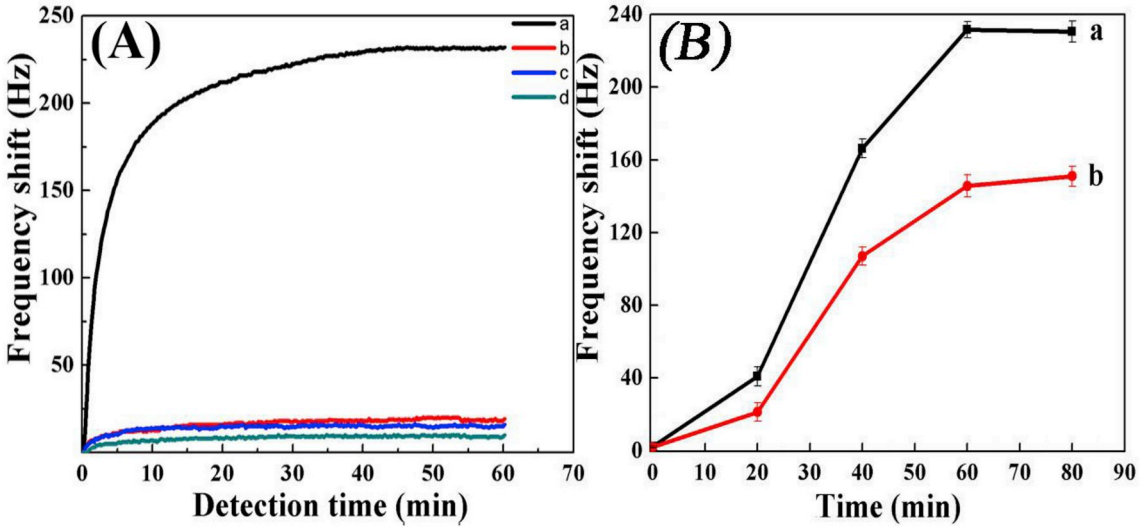

Fig. 3. (A) Frequency shift response of the MSPQC system under different conditions: 10 pM target DNA, 2.5 U/μL Exo III (curve a); 10 pM target DNA, no Exo III (curve b); no target DNA, 2.5 U/μL Exo III (curve c); no target DNA, no Exo III (curve d) (B) Effect of Exo III concentration on frequency shift response. Note: the concentration of 16S rDNA fragments was at 10 pM. Exo III concentrations were at 2.5 U/μL (curve a) and 0.5 U/μL (curve b), respectively. Error bars indicate standard deviation (n = 3).

3.4. Frequency shift response characteristics of M. tuberculosis 16S rDNA fragments

The frequency shift response of the constructed sensor to 16S rDNA fragment of *M. tuberculosis* was studied and the result was shown in Fig. 3A, When both the target and Exo III were added into the sensing system, a sizable increase in frequency shift response was observed when the time of growth of the exposed AuNPs was less than 40 min (curve a). The reason was that self-catalytic growth of the exposed AuNPs in glucose and $HAuCl_4$ solution resulted in a sharp increase in diameter of AuNPs within 40 min, thus forming conductive connection between the electrodes. The frequency shift value reached a plateau after 40 min, and prolonged time might increase the background signal. Therefore, the frequency shift value of self-catalytic growth of AuNPs at 40 min was chosen as the detection signal response value. Whereas MSPQC sensor showed almost no frequency shift responses when there was no Exo III (curve b) or target DNA (curve c), no target DNA and Exo III (curve d). The results indicated that only the presence of hybridization/Exo III incubation could initiate Exo III-assisted target recycling and cause the amplification of detection signal for *M. tuberculosis* sensor.

3.5. Effect of Exo III concentration on detection response

The frequency shift detection curves for Exo III concentrations of 2.5 U/μL (curve a) and 0.5 U/μL (curve b) were shown in Fig. 3B. As shown in Fig. 3B, it can be seen that frequency shift response increased with increasing Exo III concentration before the hybridization/Exo III incubation time was less than 60 min, and the response value reached a plateau after 60 min. The same frequency shift responses were observable with the concentrations of Exo III higher than 2.5 U/μL. To save enzyme consumption, a period of 60 min hybridization/incubation with 2.5 U/μL Exo III was sufficient for detection.

3.6. Specificity study of 16S rDNA fragment by MSPQC sensor

The specificity study of 16S rDNA fragment by MSPQC sensor was investigated by detecting five types of DNA sequences, including 16S rDNA fragment, 16S rDNA fragment with single-base, three-bases, five-bases mismatch and non-match at the same concentration. As shown in Fig. 4, the frequency shift response values for 16S rDNA fragment with single-base, three-base, five-base mismatch were only about 47.92%, 23.38% and 11.37% of that for complementary target, respectively. The non-complementary target DNA and the blank sample showed almost no frequency shift response changes. These results demonstrated the proposed method had high specificity for detection.

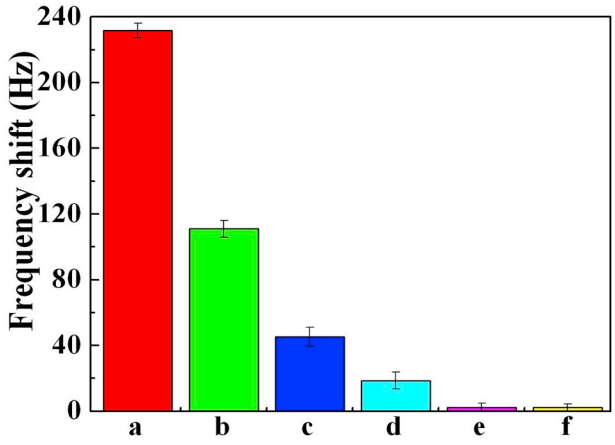

Fig. 4. The frequency shift responses of MSPQC sensor to different types of DNA sequences. (a) Complementary sequences, (b) single-base mismatched sequences, (c) three-bases mismatched sequences, (d) five-bases mismatched sequences, (e) non-complementary sequences, (f) blank in absence of target sequences. The concentration of 16S rDNA fragments was at 10 pM. Error bars indicate standard deviation (n = 3).

3.7. Detection of M. tuberculosis

3.7.1. Selectivity and repeatability detection of M. tuberculosis MSPQC sensor

M. tuberculosis H37Ra was detected by MSPQC sensor according to the procedure described in Section 2.2.1 and 2.2.3. Comparative detection were also carried out using interfering bacteria such as *E. coli*, *M. smegmatis*, *P. aeruginosa*, *S. aureus*, and *BCG*. As shown in Fig. 5, it can be seen that there was a significant frequency shift response for *M. tuberculosis* detection, while there were almost no frequency shift responses for other strains detection. In addition, the mixture samples (10^6 CFU/mL *M. tuberculosis* respectively mixed with 10^6 CFU/mL other five strains) were also detected by the proposed sensor, the frequency

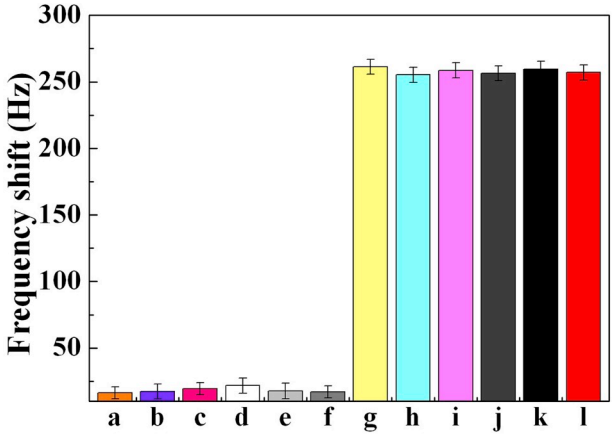

Fig. 5. The frequency shift responses to different strains. (a) The blank sample without bacteria, (b) *E. coli*, (c) *M. smegmatis*, (d) *P. aeruginosa*, (e) *S. aureus*, (f) *BCG*, (g) *M. tuberculosis,* (h) *M. tuberculosis* + *E. coli*, (i) *M. tuberculosis* + *M. smegmatis,* (j) *M. tuberculosis* + *P. aeruginosa*, (k) *M. tuberculosis* + *S. aureus*, (l) *M. tuberculosis* + *BCG*. The concentrations of these strains were at 10^6 CFU/mL. Error bars indicate standard deviation (n = 3).

shift responses of these mixed samples showed only slight changes ranging from 0.6% to 2.3% compared to the sample containing only *M. tuberculosis*. The results suggested that these strains did not interfere with the detection of *M. tuberculosis*. Therefore, the MSPQC sensor was highly selective for detection of *M. tuberculosis*.

The repeatability of MSPQC sensor was evaluated by preparing eight sensors for parallel experiment at the same conditions, and the result was showed in Table S1. The relative standard deviation (RSD) was 3.4% for detection of *M. tuberculosis* at a concentration of 10^4 CFU/mL, which indicated that the MSPQC sensor had good repeatability.

3.7.2. Detection limit of *M. tuberculosis* MSPQC sensor

The frequency shift-time response curves recorded by MSPQC system upon different concentrations of *M. tuberculosis* were illustrated in Fig. 6A. In the absence of bacteria, there was no significant frequency shift response observed (curve a). The frequency shift responses increased with the increase of *M. tuberculosis* concentration (curve b→h). As shown in Fig. 6B, the frequency shift responses exhibited a good linear relationship with the logarithm value of *M. tuberculosis* concentration within the range from 1×10^2 to 1×10^8 CFU/mL. The

Table 2
Comparison of MSPQC sensor and the culture method for 45 simulated sputum samples detection.

constructed sensor	Bacteria culture method		Total
	Positive	Negative	
Positive	13	3	16
Negative	2	27	29
Total	15	30	45

linear regression equation was $\triangle F = 53.88 + 36.54 \log C$, $R^2 = 0.987$. The RSD values showed in Table S2 were in the range of 1.8%–4.6% (n = 3). The detection time was less than 3 h. The LOD was 20 CFU/mL, which was defined as LOD = 3 × (SD/k), where SD was the standard ldeviation of the frequency shift response for blank sample, and k was the slope of fitting curve in the linear region.

3.7.3. Simulated sputum samples detection

A total of 45 simulated sputum samples were prepared and detected by MSPQC sensor according to the procedure described in Section 2.2.2 and 2.2.3. The results were compared with traditional culture methods. As shown in Table 2, among 15 positive samples, 2 samples were not detected by MSPQC sensor presumably due to the unsuccessful DNA extraction or bacterial contamination during culture. Among the negative samples, the results of 3 samples were positive using MSPQC sensor. The inconsistency between the results of two methods was associated with the low concentration (less than 10^3 CFU/mL) of *M. tuberculosis* in the samples or slow growth of *M. tuberculosis*. According to the McNemar test, no obvious change was existed between the two methods ($P = 1.0 > 0.05$). Compared to conventional culture method, the detection sensitivity and specificity of the MSPQC sensor were 86.6% (13/15) and 90.0% (27/30), respectively. Moreover, for detection of *M. tuberculosis*, conventional culture method required 4–6 weeks to yield the result, while by MSPQC sensor the detection time could be shortened to less than 3 h, thereby facilitating clinical *M. tuberculosis* diagnosis.

3.8. Comparison of the proposed sensor and other detection methods for detection of *M. tuberculosis*

The comparison of the proposed sensor with other detection methods for detection of *M. tuberculosis* was showed in Table 3. As

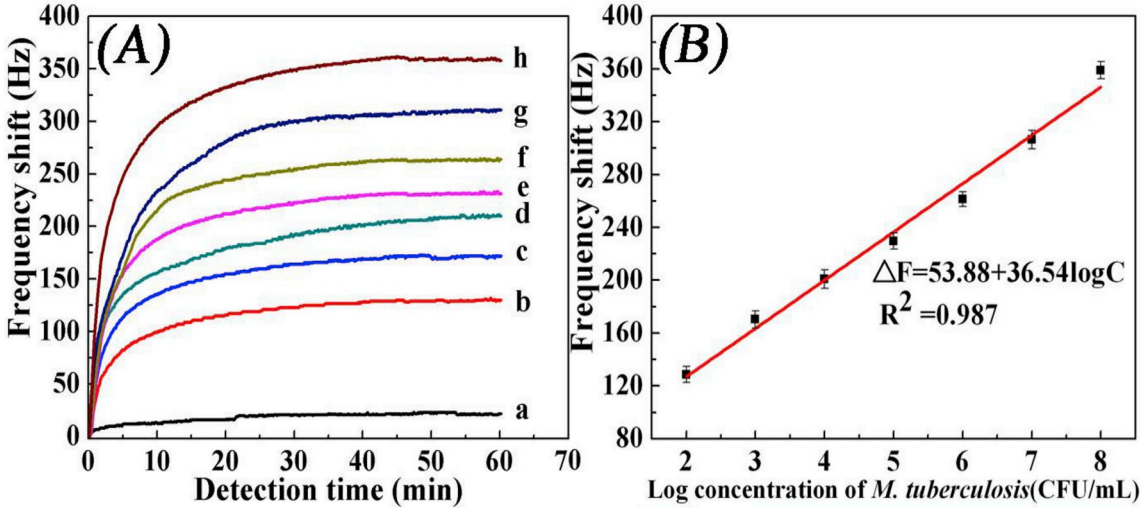

Fig. 6. (A) The frequency shift-time response curves for different concentrations of *M. tuberculosis* (a) 0, (b)1×10^2, (c) 1×10^3, (d)1×10^4, (e)1×10^5, (f)1×10^6, (g)1×10^7, (h)1×10^8 CFU/mL of *M. tuberculosis*. (B) The frequency shift response fitting curve of MSPQC sensor at different concentration of *M. tuberculosis* (CFU/mL). Error bars indicate standard deviation (n = 3).

Table 3
Comparison of the proposed sensor method with other reported methods for *M. tuberculosis* detection.

Detection technique	Specificity	Detection Time (h)	Linear range (CFU/mL)	LOD (CFU/mL)	Response target	Ref.
Bacteria culture	no	> 720	/	/	count colony	Ko et al. (2017)
BACTEC system	no	240	/	sensitivity of 81.5%	O_2	Cruciani et al. (2004)
Real-Time PCR	low	/	5–5 × 10^7	5	DNA	Leung et al. (2018)
SPR	yes	/	/	10^4	Ag85 protein	Trzaskowski et al. (2018)
Immunoassays	yes	2	10–10^8	10^3	antibody	Yang et al. (2015)
Fluorescence	yes	1	/	10	BlaC enzyme	Cheng et al. (2014)
Colorimetry	yes	5	10^4–10^7	10^4	aptamer	Li et al. (2018)
Flow cytometry	yes	2	/	3.5 × 10^3 cells/mL	antibody	Qin et al. (2008)
MSPQC	yes	30	/	100	$NH_3 + CO_2$	Mi et al. (2012)
MSPQC	no	48–192	10^2–10^7	10	$NH_3 + CO_2$	Ren et al. (2008)
Proposed method	yes	< 3	10^2–10^8	20	DNA	

shown in Table 3, the sensitivity of the proposed sensor was comparable with other *M. tuberculosis* detection methods. Several methods such as real-time PCR, SPR, fluorescence and flow cytometry resulted in high sensitivity in less time. However, these methods required costly centralized laboratories. The targets of other methods used culture metabolites or antibodies, which cannot overcome the shortcomings of long culture time or expensive antibodies. While the proposed sensor had advantages of high sensitivity, low cost and label-free property, *M. tuberculosis* could be detected quickly. Therefore, the proposed sensor held a great potential for the development of an ultrasensitive biosensing platform for early diagnosis of *M. tuberculosis*.

4. Conclusions

A rapid, simple, inexpensive, and label-free 16S rDNA MSPQC sensor that detected *M. tuberculosis* with a combination of Exo III-aided target recycling was developed. The proposed sensor exhibited high sensitivity and specificity for detection of *M. tuberculosis*, where the LOD was 20 CFU/mL and the detection time was less than 3 h. Detection of real samples in patients will be our further work. The method offers a new approach for rapid detection of *M. tuberculosis* and has potential application in the clinical diagnosis of *M. tuberculosis*.

Declaration of interests

The authors declare that they have no known competing financialinterestsor personal relationships that could have appeared to influence the work reported in this paper.

CRediT authorship contribution statement

Jialin Zhang: Conceptualization, Methodology, Formal analysis, Investigation, Writing - original draft. **Ji Huang:** Formal analysis. **Fengjiao He:** Supervision, Writing - review & editing, Resources, Project administration, Funding acquisition.

Acknowledgements

This research work was supported by the National Natural Science Foundation of China (No. 21275042).

Appendix A. Supplementary data

Supplementary data to this article can be found online at https://doi.org/10.1016/j.bios.2019.111322.

References

Chen, Y.H., Guo, S.L., Zhao, M., Zhang, P., Xin, Z.L., Tao, J., Bai, L.J., 2018a. Biosens. Bioelectron. 119, 215–220.
Chen, Y.H., Duong, H., Wen, S.H., Mi, C., Zhou, Y.Z., Shimoni, O., Valenzuela, S.M., Jin, D.Y., 2018b. Anal. Chem. 90, 663–668.
Cheng, Y.F., Xie, H.X., Sule, P., Hassounah, H., Graviss, E.A., Kong, Y., Cirillo, J.D., Rao, J.H., 2014. Angew. Chem. 126, 9514–9518.
Chu, Z.J., Xiao, S.J., Liu, Y.H., Xiong, G.L., Huang, D.J., Wang, S.P., Zhao, X.J., Zhang, Z.B., 2019. Sensor. Actuator. B Chem. 282, 904–909.
Chung, H.J., Castro, C.M., Im, H., Lee, H., Weissleder, R., 2013. Nat. Nanotechnol. 8, 369–375.
Comotti, M., Pina, C.D., Matarrese, R., Rossi, M., 2004. Angew. Chem. Int. Ed. 43, 5812–5815.
Cruciani, M., Scarparo, C., Malena, M., Bosco, O., Serpelloni, G., Mengoli, C., 2004. J. Clin. Microbiol. 42, 2321–2325.
Das, J., Ivanov, I., Safaei, T.S., Sargent, E.H., Kelley, S.O., 2018. Angew. Chem. 130, 3773–3778.
Gao, Y., Li, B.X., 2013. Anal. Chem. 85, 11494–11500.
Gupta, S., Kakkar, V., 2018. Biosens. Bioelectron. 115, 14–29.
Hünniger, T., Felbinger, C., Wessels, H., 2015. J. Agric. Food Chem. 63, 4291–4296.
He, F.J., Xiong, Y.C., Liu, J., Tong, F.F., Yan, D.Y., 2016. Biosens. Bioelectron. 77, 799–804.
Ko, Y., Kim, C., Chang, B., Lee, S.Y., Park, S.Y., Mo, E.K., Hong, S.J., Lee, M.G., Hyun, I.G., Park, Y.B., 2017. Tuberc. Respir. Dis. 80, 35–44.
Lakshmanan, R.S., Efemov, V., Cullen, S.M., Killard, A.J., 2014. Sensor. Actuator. B Chem. 192, 23–28.
Li, F., Yu, Y.Q., Li, Q., Zhou, M., Cui, H., 2014. Anal. Chem. 86, 1608–1613.
Li, L., Liu, Z.G., Zhang, H., Yue, W.Q., Li, C.W., Yi, C.Q., 2018. Sensor. Actuator. B Chem. 254, 337–346.
Leung, K., Siu, G., Tam, K., Ho, P., Wong, S., 2018. Tuberculosis 112, 120–125.
Lu, L.H., Su, H.J., Li, F., 2017. Anal. Chem. 89, 8328–8334.
Mi, X.W., He, F.J., Xiang, M.Y., Lian, Y., 2012. Anal. Chem. 84, 939–946.
N'guessan, K., Horo, K., Coulibaly, I., Adegbele, J., Kouame-Adjei, N., Seck-Angu, H., Dosso, M., 2016. Int. J. Mycobacteriol. 5, S164–S165.
Qin, D.L., He, H.H., Wang, K.M., Tan, W.H., 2008. Biosens. Bioelectron. 24, 626–631.
Qu, X.M., Zhu, D., Yao, G.B., Su, S., 2017. Angew. Chem. 129, 1881–1884.
Ren, J.L., He, F.J., Yi, S.L., Cui, X.Y., 2008. Biosens. Bioelectron. 4, 403–409.
Shi, C., Xu, Q., Ge, Y., Jiang, L., Huang, H., 2017. J. Agric. Food Chem. 65, 6674–6681.
Shi, X.H., Zhang, J.L., He, F.J., 2019. Biosens. Bioelectron. 132, 224–229.
Sypabekova, M., Jolly, P., Estrela, P., Kanayeva, D., 2019. Biosens. Bioelectron. 123, 141–151.
Trzaskowski, M., Napiorkowska, A., Ciach, T., 2018. Sensor. Actuator. B Chem. 260, 786–792.
World Health Organization (WHO), 2016. Global Tuberculosis Report. Available at: http://apps.who.int/iris/bitstream/10665/250441/1/9789241565394-eng.pdf.
Wang, H.Y., Du, P.C., Li, J., Zhang, Y.Y., Zhang, W., Han, N., Woo, P., Chen, C., 2014. J. Med. Microbiol. 63, 433–440.
Xiong, E.H., Zhang, X.H., Liu, Y.Q., Zhou, J.W., Y, P., Li, X.Y., Chen, J.H., 2015. Anal. Chem. 87, 7291–7296.
Yan, L.P., Zhang, Q., Xiao, H.P., 2017. BMC Infect. Dis. 17, 545.
Yang, H., Qin, L.H., Wang, Y.L., 2015. Int. J. Nanomed. 10, 77–88.
Zhang, P., Guo, X.L., Wang, H.H., Sun, Y., Kang, Q., Shen, D.Z., 2017. Sens. Actuators B:Chem. 248, 551–559.
Zhou, F.L., Li, B.X., 2015. Anal. Chem. 87, 7156–7162.
Zheng, X.X., Liu, Q., Jing, C., Li, Y., Li, D., Luo, W.J., Wen, Y.Q., He, Y., Huang, Q., Long, Y.T., Fan, C.H., 2011. Angew. Chem. 50, 11994–11998.